

See discussions, stats, and author profiles for this publication at: <https://www.researchgate.net/publication/339781033>

# Proposed Design Guideline of Dynamic Compaction for Practicing Engineers

Conference Paper · August 2017

---

CITATIONS

0

READS

1,424

1 author:



Tjie-Liong Gouw Dr.  
Universitas Katolik Parahyangan

75 PUBLICATIONS 119 CITATIONS

[SEE PROFILE](#)

Some of the authors of this publication are also working on these related projects:



ground improvement [View project](#)



Deep excavations [View project](#)

# GEOTECHNICAL ENGINEERING

Journal of the



AGSSEA  
ASSOCIATION OF GEOTECHNICAL  
SOCIETIES IN SOUTHEAST ASIA

Sponsored by



**EDITORS: NOPPADOL PHIENWEJ, SUTTISAK SORALUMP, APINITI  
JOTISANKASA, SUCHED LIKITLERSUANG AND TIRAWAT BOONYATEE  
CONVENORS: SAN SHYAN LIN, GEOFF CHAO AND OOI TEIK AUN**

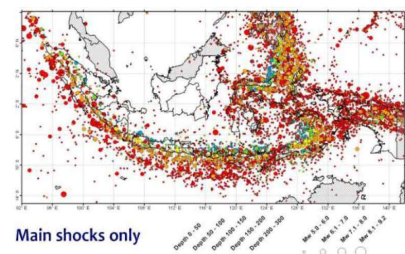


Figure 1: Proposed Design Guideline of Dynamic Compaction for Practicing Engineers  
(After Tjie-Liong GOUW, 2018)



Figure 2: Recent Development on Soft Ground Tunnelling  
(After Mitsutaka Sugimoto, Hideyuki Tanaka, Ngoc Thi Huynh, Salisa Chaiyaput, Le Gia Lam, and Jian Chen, 2018)

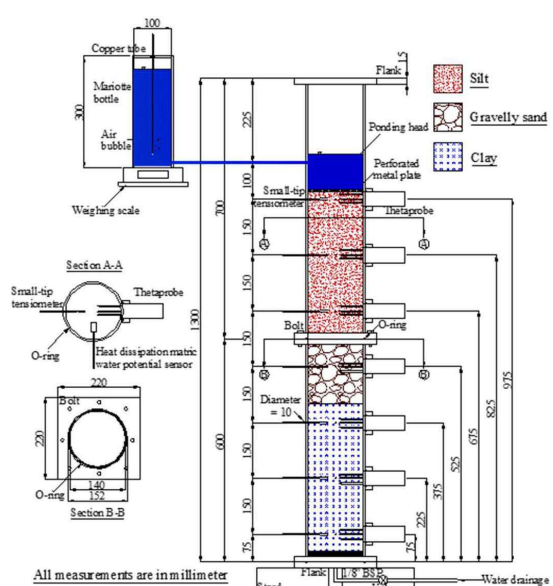


Figure 9: Schematic diagram of the soil column: State-of-the-Art Research in Geo-energy and Geo-environmental Engineering:  
Energy Pile and Earthen Capillary Landfill Cover System  
(After Charles W.W. Ng, Jason L. Coo & Anthony Gunawan, 2018)

**Noppadol Phienwej, Suttisak Soralump, Apiniti Jotisankasa, Suched Likitleruang  
and Tirawat Boonyatee**

**TABLE OF CONTENTS**

<u>List of Papers</u>	<u>Page</u>
<b>1:</b> State-of-the-Art Research in Geo-energy and Geo-environmental Engineering: Energy Pile and Earthen Capillary Landfill Cover System <i>By Charles W.W. Ng, Jason L. Coo &amp; Anthony Gunawan</i> <a href="#">***Please click here to download paper</a>	1-11
<b>2:</b> Validation of a New Simplified Hypothesis B Method for Calculating Consolidation Settlement of Clayey Soils Exhibiting Creep <i>By J.-H. Yin and W.-Q. Feng</i> <a href="#">***Please click here to download paper</a>	12-21
<b>3:</b> Finite Element Analysis to Characterize the Lateral Behaviour of a Capped Pile Group <i>By Chao-Kuang Hsueh, San-Shyan Lin and Dominic E. L. Ong</i> <a href="#">***Please click here to download paper</a>	22-31
<b>4:</b> Proposed Design Guideline of Dynamic Compaction for Practicing Engineers <i>By Tjie-Liong Gouw</i> <a href="#">***Please click here to download paper</a>	32-40
<b>5:</b> Settlement of River Dykes and Their Adjacent Residences on Soft Clay Deposits After the Tohoku-Pacific Ocean Earthquake in 2011 <i>By K. Yasuhara, S. S. Yang, I. Horikawa and H. Yamane</i> <a href="#">***Please click here to download paper</a>	41-48
<b>6:</b> Application of Photogrammetry and Image Analysis for Rock Slope Investigation <i>By D-H. Kim, A. S. Balasubramaniam and I. Gratchev</i> <a href="#">***Please click here to download paper</a>	49-56
<b>7:</b> Longitudinal and Transverse Interactions between Stacked Parallel Tunnels Constructed using Shield Tunnelling in Residual Soil <i>By C.W. Boon and L.H. Ooi</i> <a href="#">***Please click here to download paper</a>	57-71
<b>8:</b> Common Blind Spots in Ground Investigation, Design, Construction, Performance Monitoring and Feedbacks in Geotechnical Engineering. <i>By Shaw Shong Liew</i> <a href="#">***Please click here to download paper</a>	72-84
<b>9:</b> Detrimental Effects of Lateral Soil Movements on Pile Behaviour <i>By D.E.L. Ong</i> <a href="#">***Please click here to download paper</a>	85-95
<b>10:</b> Optimising Cement Dosage in Ground Improvement and Early Quality Control Schemes <i>By S.C. Chian</i> <a href="#">***Please click here to download paper</a>	96-103
<b>11:</b> Effects of Preloading of Struts on Retaining Structures in Deep Excavations <i>By Richard N. Hwang and Lup-Wong Wong</i> <a href="#">***Please click here to download paper</a>	104-114
<b>12:</b> Anchors of Anchored Slopes in Taiwan <i>By Hung-Jiun Liao, Shih-Hao Cheng and Chun-Chung Chen</i> <a href="#">***Please click here to download paper</a>	115-122
<b>13:</b> Hexagonal Wire Mesh Panel Tensile Behaviour due to Weaving Patterns <i>By Chiwan Hsieh, Zhi-Yao Cai, and Wen-Shin Shuy</i> <a href="#">***Please click here to download paper</a>	123-130

<b>14:</b> Trenchless Excavations for Underground Pipelines in Difficult Geology <i>By Keh-Jian Shou, Jonas Yen, and Chih-Ying Hsieh</i> <a href="#">***Please click here to download paper</a>	131-135
<b>15:</b> Liquefaction-Induced Settlement of Structures on Shallow Foundation <i>By C.W. Lu, L. Ge, M.C. Chu, and C.T. Chin</i> <a href="#">***Please click here to download paper</a>	136-139
<b>16:</b> Evaluation of Failure of Embankment Slope Constructed with Expansive Soils <i>By Kuo Chieh Chao, Jong Beom Kang and John D. Nelson</i> <a href="#">***Please click here to download paper</a>	140-149
<b>17:</b> Strength and Stiffness Parameters of Bangkok clays for Finite Element Analysis <i>By Suched Likitlersuang, Chhunla Chheng, Chanaton Surarak and Arumugam Balasubramaniam</i> <a href="#">***Please click here to download paper</a>	150-156
<b>18:</b> Failure of Riverbank Protection Structure and Remedial Approach <i>By S. Horpibulsuk, A. Udomchai, M. Hoy, A. Chinkulkijniwat, and D. B. Van</i> <a href="#">***Please click here to download paper</a>	157-163
<b>19:</b> Recent Developments of Soft Ground Improvements using Prefabricated Vertical Drains (PVD) and Deep Cement Mixing (DCM) <i>By D.T. Bergado, A.S. Balasubramaniam and P.V. Long</i> <a href="#">***Please click here to download paper</a>	164-181
<b>20:</b> Study on Shield Operation Method in Soft Ground by Shield Simulation <i>By Mitsutaka Sugimoto, Hideyuki Tanaka, Ngoc Thi Huynh, Salisa Chaiyaput, Le Gia Lam, and Jian Chen</i> <a href="#">***Please click here to download paper</a>	182-191

### Cover Photographs

Figure 1: Proposed Design Guideline of Dynamic Compaction for Practicing Engineers  
(After Tjie-Liong GOUW, 2018)

Figure 2: Recent Development on Soft Ground Tunnelling  
(After Mitsutaka Sugimoto, Hideyuki Tanaka, Ngoc Thi Huynh, Salisa Chaiyaput, Le Gia Lam, and Jian Chen, 2018)

Figure 9: Schematic diagram of the soil column: State-of-the-Art Research in Geo-energy and Geo-environmental Engineering: Energy Pile and Earthen Capillary Landfill Cover System  
(After Charles W.W. Ng, Jason L. Coo & Anthony Gunawan, 2018)

## GEOTECHNICAL ENGINEERING

### Paper Contribution, Technical notes and Discussions

SEAGS & AGSSEA encourage the submission of scholarly and practice-oriented articles to its journal. The journal is published quarterly. Both sponsors of the journal, the Southeast Asian Geotechnical Society and the Association of Geotechnical Societies in Southeast Asia,

# Proposed Design Guideline of Dynamic Compaction for Practicing Engineers

Tjie-Liong Gouw  
*Senior Geotechnical Consultant, Jakarta, Indonesia*  
*E-mail: gtloffice@gmail.com*

**ABSTRACT:** During an earthquake, saturated fine sands tends to lose its bearing capacity due to the earthquake induced and accumulated excess pore water pressure. The phenomenon, known as liquefaction, is one of the earthquake hazards that need to be mitigated in an earthquake prone area such as the archipelagos of Indonesia. The occurrence of an earthquake cannot be prevented and, with the present knowledge, is difficult - if not impossible - to predict. However, liquefaction potential can be mitigated by carrying out proper ground improvement methods. The most common ground improvement schemes that have been widely implemented in mitigating liquefaction potential of saturated fine sands in Indonesia are dynamic compaction and vibro-compaction. However, many practicing engineers are still not familiar with the methods. This paper presents the design, execution, and evaluation methods of dynamic compaction. Two case histories on real projects are also presented as examples.

**KEYWORDS:** Dynamic compaction, Design guideline

## 1. INTRODUCTION

One of the geotechnical problems in Indonesia, a country of thousands islands, is: it lies right at the ring of fire, indicating high occurrence of earthquake and volcanic activities (Figure 1). Adding to the high seismicity problem, many of its coastal regions also lie on saturated loose fine sandy soils. Combination of high seismicity and saturated loose fine sandy soils lead to high potential occurrence of liquefaction, a phenomenon where the sandy soil loses its bearing capacity due to the accumulation of earthquake induced pore water pressure,  $u$ . Once the accumulation of pore water pressure equals or exceeds the total overburden pressure,  $\sigma_v$ , of the sandy ground, the effective stress,  $\sigma'_v$ , becomes zero and the soil loses its shear strength. Loss of shear strength causes the soil to liquefy and to completely lost its bearing capacity, hence the structures above will damage or even collapse. To mitigate the liquefaction potential, saturated loose fine sandy soils need to be improved by compacting them up to a certain degree.

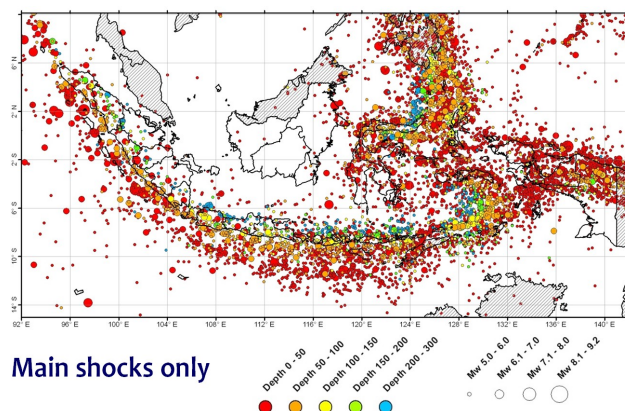


Figure 1 Indonesia in the Ring of Fire (Irsyam, 2012)

Figure 2 shows various available ground improvement techniques and its suitability for broad category of soils. It can be seen that a number of techniques can be applied to improve sandy soils, e.g. blasting, dynamic compaction, vibro-compaction, certain type of grouting and deep mixing. This paper only presents the ground improvement by dynamic compaction, starting from design / planning, execution, instrumentations, monitoring, up to evaluation of the improvement results. Some case histories will also be presented.

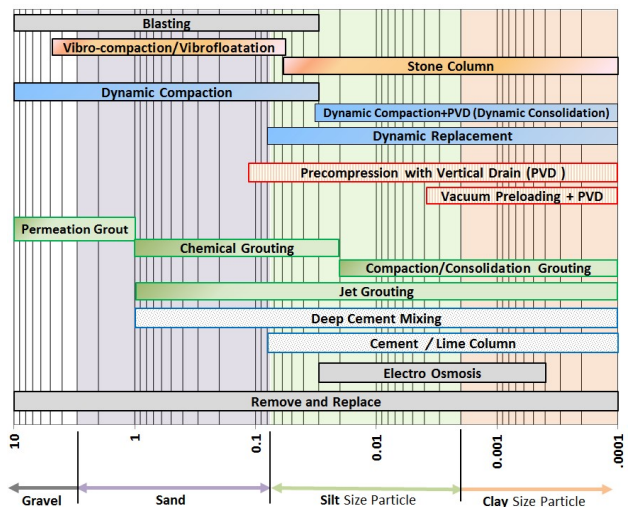


Figure 2 Various Ground Improvement Methods (Modified after Soletanche Bachy Technical Guide, 2011)

## 2. LIQUEFACTION POTENTIAL

Dynamic compaction and vibro-compaction techniques are often adopted to mitigate liquefaction potential of sandy soils. In order to warrant the success of the adopted improvement techniques, a proper assessment of liquefaction potential is of utmost important. Method to analyse the liquefaction potential shall not be elaborated in this paper, readers may refer to the references published elsewhere, among others are: Seed and Idriss (1971, 1982), Seed et al (1985), Ishihara (1985), Stark and Olson (1995), Andus and Stokoe (2000); Cetin et al (2004), Idriss and Boulanger (2004).

## 3. DYNAMIC COMPACTION

Compaction is defined as the process of soil densification by used of external compaction effort. Dynamic compaction is a ground improvement method where in situ soil is densified by repeatedly and systematically dropping a heavy weight (tamper or pounder) from a certain height. The weight of the pounder ranges from 8 to 200 metric tons, and the drop height varies from 10 to 40 meters. This method is first pioneered by Louis Menard in the early seventies (Gambin, 1979, Menard and Broise, 1975). Figure 3 shows the dynamic compaction equipment and process.

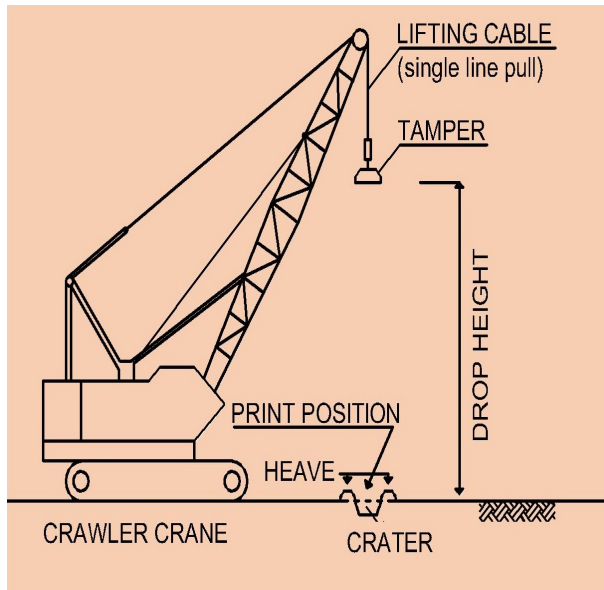


Figure 3 Dynamic Compaction Equipment and Process

This method is primarily suitable for cohesionless or granular soils, be it saturated or unsaturated. It is also suitable to compact fill materials that consist of stones, gravels, industrial and domestic waste. However, it is not suitable to be directly applied in cohesive soils without any modification. To improve cohesive soil it needs modification, e.g. by spreading gravel blanket on top of the ground surface and then tampering / pounding / hammering it into the ground to form gravel columns; or by installing prefabricated vertical drain into the cohesive soils and then pounding the tamper onto the ground, the pounding will induce excess pore water pressure which will then dissipate through the vertical drain and causing the soil to consolidate.

When the pounder hits the ground, it generates three types of waves as illustrated in Figure 4 (Gambin, 1979), and elaborated below:

- The fastest among the three is the compression wave, also known as P-wave. It can travel through soil solids and groundwater. Being the fastest it will arrive first at every point in the soil body. This P-wave creates push and pull actions onto the soil structures (Figure 5) and hence breaks the interlocking effects among the soil particles. In saturated non cohesive soils, the compression wave increases the pore water pressure which in turn breaks the interlocks among the soil particles.
- The second wave that arrives at the soil elements is the shear or distortional wave, also known as S-wave, which is slower than P-wave. The S-wave travels only in soil solids; it causes the soil particles to slide against one another to a denser state (Figure 5).
- The last wave, the slowest and the last wave arrives at the soil elements among the three waves generated, is the Rayleigh wave. The Rayleigh wave travels at and near the ground surface, in a cylindrical wave front; it also causes the soil particles to slide against one another to a denser state.

Menard (1975), explained the compaction mechanism in saturated sandy soils as presented in Figure 6. The first diagram in Figure 6 shows accumulation of compaction energy over time (induced by repeated blows onto the ground surface). The second diagram shows soils volume compression caused by the accumulated compaction energy. The third diagram shows the increasing pore water pressures induced by the accumulated pounding energy, until it reaches maximum, indicating further blows will no longer effective. The excess pore water pressure dissipated

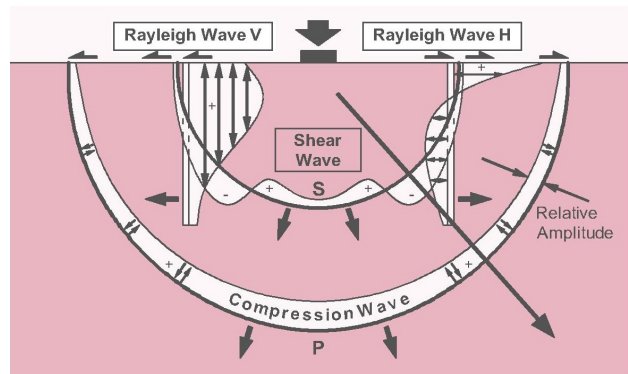


Figure 4 Waves Generated when Ponder Hits the Ground  
(after Gambin, 1979)

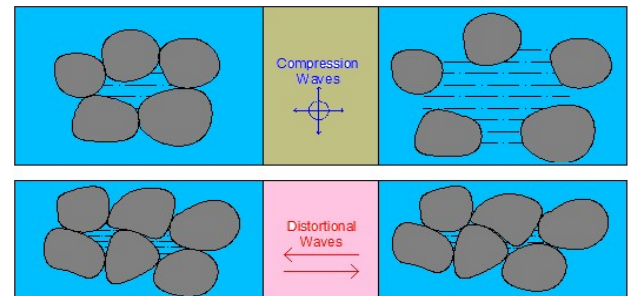


Figure 5 Compaction Mechanisms in Saturated Granular Soils

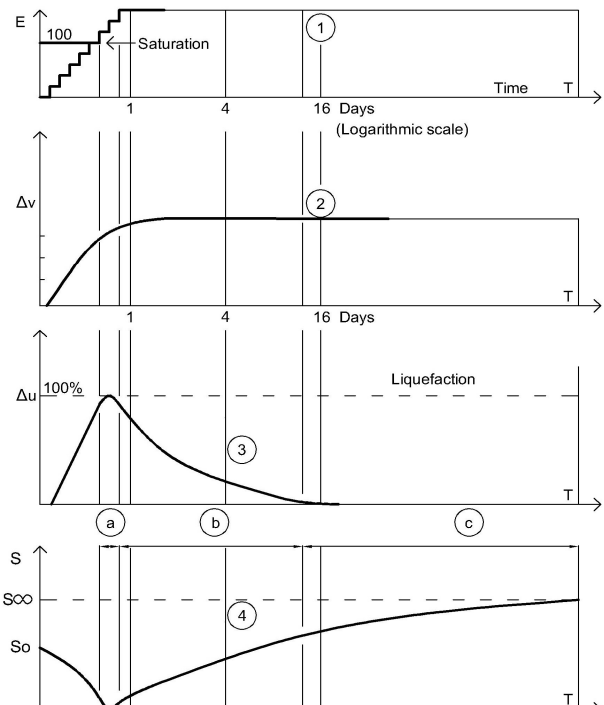


Figure 6 Compaction Mechanisms (after Menard, 1975)

with the passage of time, and hence the soil consolidates toward a denser state. The fourth diagram shows the accumulated excess pore water pressure causing the soil to liquefy (segment a in the diagram) and lost its shear strength, when the blow is stopped, excess pore water pressures dissipates and the soil starts to gain its shear

strength (segment b) to a higher state. Menard also said thixotropic effect will cause the soil to have even higher shear strength (segment c).

### 3.1 Design

Dynamic compaction design is started by determining the required depth to be improved. The purpose of the treatment is the governing factor in determining the required improvement depth. Based on the author's experiences, the following guidelines can be adopted:

- To mitigate foundation settlement problems, the depth of improvement must be up to the depth where the stresses induced by the structures are only 5% of the stresses exerted at the base of the structure foundation, or until the depth where the settlement of the untreated deeper layers is no longer detrimental.
- To mitigate soil liquefaction problems of structures founded on shallow foundation, the improvement can be carried up to a depth in such a way that when the underlying unimproved ground liquefy during earthquake, the improved upper soil layer will not liquefy and only minimal impact appear at the ground surface. Ishihara chart (Ishihara, 1995) presented in Figure 7 can be used to determine the required improvement depth.
- To mitigate soil liquefaction problems of structures built on pile foundation, the improvement depth has to extend to the depth of all liquefiable soil layers where the pile foundation existed. This is to assure that the piles will not buckle if the soil liquefies.

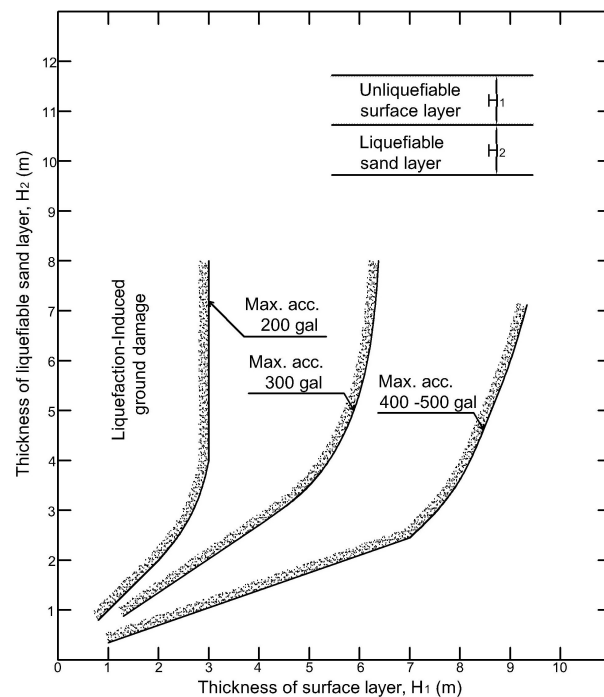


Figure 7 Thickness of Unliquefiable Surface Layer Recorded when Underlying Liquefied Sand Layer induced Minimal Damages at the Ground Surface (Ishihara, 1995)

Once the required improvement depth, D, is determined, the next step is to estimate the pounder weight, height of drop, and cumulated energy necessary to achieve the target improvement depth. The weight and the drop height of pounder shall be estimated by using the following empirical formula:

$$D = n \sqrt{MH} \quad (1)$$

where D is the target improvement depth (m), M is the pounder mass (ton), H is the height of drop (m), and n is an empirical factor varying from 0.3 to 1.0. A guideline on the n values, derived from many case histories, is given in Table 1. With this equation the value of MH can be calculated. The next step is to decide the weight of the pounder; it generally varies from 5 to 40 ton, with contact pressures of 4 to 8 ton/m<sup>2</sup>. Concurrently, the height of drop is determined; generally within 10 to 30m.

Table 1 Empirical Dynamic Compaction n Factor

Soil Type	Degree of Saturation	n
All Soils		0.50
Pervious Soil Deposits - Granular Soil	High	0.50
	Low	0.50 - 0.60
Semi Pervious Soil Deposits Primarily Silts with PI < 8	High	0.35 - 0.40
	Low	0.40 - 0.50
Impervious Pervious Deposits Primarily Clayey Soils with PI > 8	High	Not recommended
	Low	0.35 - 0.40
Fine Sand		0.65
Soft clay**		0.66
Loess**		0.55
Silty sand		0.65
Municipal Waste		0.35
Clayey Sand		0.50
Soil with unstable structure		0.50
Silts and sands		0.67
Pure frictional soils		1.00
Sand with Fines < 15%	High	0.80
Coralline Silty Sand with Fines < 35%	High	0.35

after: Gouw (1989), Gouw et al (2013), Qian (1986), Lukas (1995), Smoltczyk (1983), Van Impe (1989)

\*\* from Qian(1986), caution suggested as the n values appear to be very high. Generally, saturated soft clay and loess cannot be compacted without any additional measures.

Next, the cumulative energy required to compact an area up to a certain depth can be estimated through Table 2. Multiply the cumulative energy, E<sub>c</sub>, obtained from Table 2 with the target improvement depth, D, to get the estimated average energy required for improving a certain area of ground,

$$E_a = E_c \times D \quad (2)$$

The estimated number of blows required to densify per unit area of the ground is determined by:

$$\begin{aligned} N_{\text{unit area}} &= E_a / (M H) \\ &= (E_c D) / (M H) \end{aligned} \quad (3)$$

The poundings are normally carried out in a square grid pattern with every pounding point centre to centre distance of S. Note that

the pounding point is usually termed as print. The distance S is generally adopted within 1.5 to 4 times pounder diameter. Hence, the total number of blows at every print is:

$$N_{\text{print}} = S \times S \times N_{\text{unit area}} \quad (4)$$

Table 2 Empirical Dynamic Compaction Cumulative Energy,  $E_c$

Type of deposit	Applied energy (t.m/m <sup>3</sup> )
Pervious coarse grained soil	20-25
Semi-pervious fine grained soils, clay fills above water table	25-35
Saturated Coralline Silty Sand (fines 15-35%) **	59
Landfills	60-110

Remarks:

- Use higher value for loose soil deposit
- Use higher value for recently placed fills (less than 3-5 years)
- Applied energy is obtained by multiplying the values by the depth of treatment
- Applied energy of the standard compaction test is 56 t.m/m<sup>3</sup>

after: Gouw (1989), Gouw et al (2013), Lukas (1995)

In actual dynamic compaction execution, the number of N blows calculated above shall not be carried out at one go. At every print point, the pounding is stopped when the cumulative blow energy has reached saturated stage. The pounding saturated stage is defined as follows:

- When the depth of the crater created by the blows has reached the height of the pounder plus 25cm. This is meant for the ease of pulling up the pounder out of the crater.
- When the ground around the print started to show heaving phenomenon. This is normally due to the increase of pore water pressure.

Note that in practice, the number of blow per print is determined from heave and penetration test as shown in the next section, a and b serve as general guide only. In case a, the blow can be directly restarted after the crater is backfilled or flatten out. In case b, the blow is restarted when the excess pore water pressure has been dissipated and the crater is backfilled or level out. This second stage of pounding series is restarted/repeated at the same print point as the previous stage, the pounding series is named as pass two, while the previous series of blows is named as pass one. Subsequent stages of blows on the same print points, if any, are named accordingly.

Examples: Assumed treatment to be done on saturated sand layer with fine content less than 15%, target depth of improvement, D is 16 m. From Table 1, the value of n is 0.8, so:

$$MH = (D/n)^2 = (16/0.8)^2 = 400 \text{ ton m}$$

take a drop height of H = 25 m

then M = 16 ton

Take pounder base area of 2 m x 2 m

$$\text{Height of pounder} = 400 / (2 \times 2 \times 7.8) = 0.52 \text{ m}$$

From Table 2, the cumulative required,  $E_c$ , is estimated to be around 20 t.m/m<sup>3</sup>. Hence, the number of blows required to densify a every square meter of ground is:

$$N_{(1m \times 1m)} = (E_c D) / (M H)$$

$$= (20 \times 16) / 400 = 0.8 \text{ blows/m}^2$$

If the minimum centre to centre pounding distance of 2 times diameter (width) of the pounder is adopted, i.e. 2 x 2m = 4 m, then every print point will require a total blow of:

$$N_{\text{print}} = 4m \times 4m \times 0.8 \text{ blows/m}^2 \approx 13 \text{ blows/print}$$

In practice, the pounding is not directly applied in one phase with 4m x 4m distance, but spread over two phases or more. If the poundings are spread over two phases, then the execution pattern shall be as presented in Figure 8. Every print is still subjected to estimated total blows of 13 blows/print.

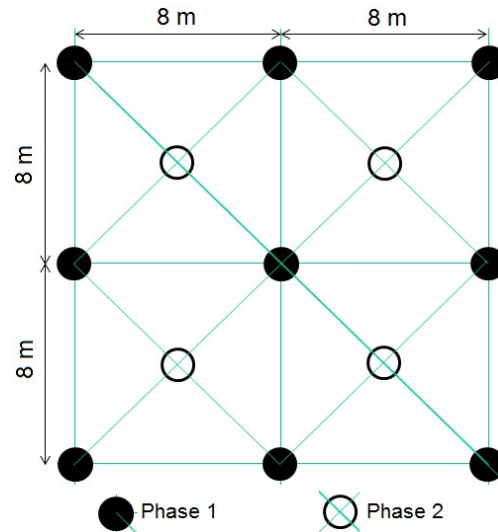


Figure 8 Pounding in Two Phases

### 3.2 Execution and Testing

Dynamic compaction equipment is relatively simple (Figure 9). It only needs a lifting crane able to lift and to drop the pounder from the design height; a bulldozer to backfill and level out the created print craters; and a pounder of a certain weight and contact area. In the older days, the crane must be able to lift and drop the pounder using only a single line pulling wire. However, to date an automatically trigger release mechanism to drop the pounder from its design height eliminates the need of single line crane.

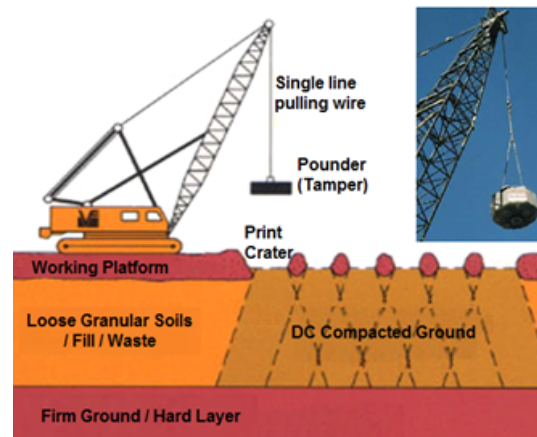


Figure 9 Dynamic Compaction Equipment

Execution of dynamic compaction work is often started with a trial area to verify the design, especially when the job is carried out on soil layers where there is no prior similar experience. The minimum size of the trial area is  $2D \times 2D$  square grid, where  $D$  is the depth to be treated. The first phase of the trial compaction square grid distance is usually taken equal with the depth to be treated, i.e.  $D \times D$ ; if  $D$  exceeds 10 m, the distance can be reduced to  $0.5D \times 0.5D$ . The minimum print distance is 1.5 pounder diameter (width). Figure 10 shows a trial compaction area executed in three phases of poundings.

Example: Say the planned treated depth,  $D = 16m$ , pounder base area (contact area) is  $2m \times 2m$ .

- Select grid distance of  $S = 0.5 D = 8m$
- Phase 1: Pounding on the points determined as phase 1, indicated as black circles in Figure 10. Figure 11 shows the moment when the pounder hit the ground. Figure 12 shows the condition right after pounding.
- Repeat the pounding at the same print point. At end of every pounding measure and calculate the volume of created soil depression (crater),  $V_d$ ; Also measure and calculate the volume of soil heave around the crater,  $V_h$  (Figure 13 and 14).

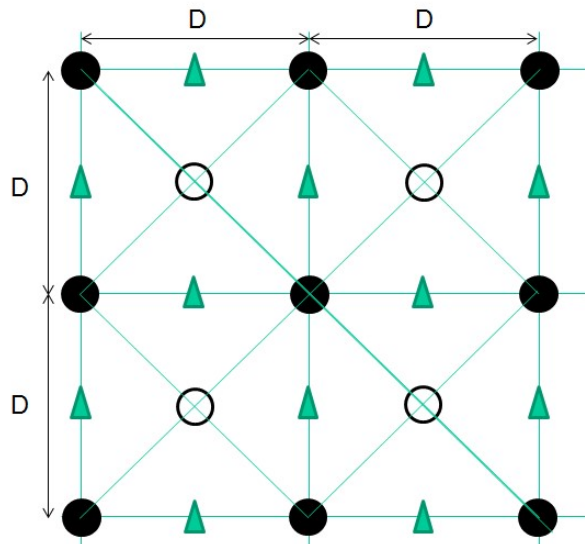


Figure 10 Three Phase Pounding Pattern



Figure 11 Moment when Pounder Hits the Ground



Figure 12 Condition Right after Pounding



Figure 13 Measurement of Crater Volume

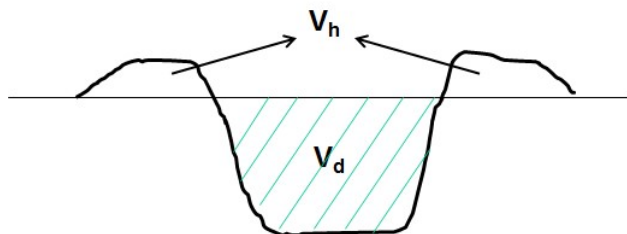


Figure 14 Volume of Soil Depression,  $V_d$ , vs Heave,  $V_h$

- Stop the pounding process when pounding efficiency (defined as net depression volume,  $V_{net} = V_d - V_h$ , divided by volume of depression,  $V_d$ ) is smaller than or equal to 40%.
 
$$E_f = (V_d - V_h) / V_d \leq 40\% \quad (5)$$
- Move to the next print position.
- After all phase 1 print points (all the black circles in Figure 10) at the trial area are pounded. Conduct in situ test (either SPT, CPT or Pressuremeter test) at the untreated point located among the print positions, and compare it with the pre-treatment SPT/CPT/Pressuremeter. Evaluate whether the target treated values has been achieved.
- If the in situ tests reveal that the compaction results have not yet achieve its target values, carry on with phase 2 poundings. The phase 2 poundings are carried out at the centre point of within phase 1 print points (empty circles in Figure 10).

- As in phase 1, measure the depression and heave volumes to determine the optimum number of blows at every print point.
- After phase 2 compaction is completed, again carry out in situ test at the untreated point located within the print points of phase 1 and phase 2. Evaluate the results.
- If phase 2 compactions still have not reached the target values, carry on with phase 3 poundings (noted as triangular in Figure 10) and repeat the whole procedures.
- At every stage, remember to always record the number of blows at every print point, the drop height, and the backfill volume added (if any).
- At every compaction phase, when the created craters make the movement of equipment difficult, the craters need to be backfilled and/or levelled out.
- Once the target design values of the treated ground has been achieved, level out all treated area. Then carry out final pounding with a drop height of only 2 to 4m. This process, commonly known as ironing tamping, is meant to further compact the ground surface layer. Finally, vibrating roller is used to compact the upper 30-50 cm surface layer as it is almost impossible to compact this upper layer using dynamic compaction equipment.
- When the whole process is completed, measure the surface elevation, compare it with the pre-treatment elevation, calculate and estimate the enforced settlement created by the dynamic compaction process (while not forgetting take into account the backfill volume added, if any).

Based on this trial tamping, decide the compaction pattern and program for the whole area to be treated. At every 500 to 1000 m<sup>2</sup> treated area, always conduct in situ test to evaluate the compaction results and the degree of improvement achieved. Also conduct surface elevation measurement to calculate the enforced settlement obtained.

Degree of improvement achieved normally depends on:

- Thickness of the soil treated
- Type and characteristics of the soil
- Groundwater elevation
- Pre-treatment density or consistency

Typical degree of improvement and maximum bearing capacity achieved is presented in Table 3.

Table 3 Typical Degree of Improvement by Dynamic Compaction

Soil Type	Degree of Improvement	Maximum Bearing Capacity Achieved
Clay (unsaturated)	100 - 150%	100 kPa
Silt	200%	200 kPa
Sand	400%	350 kPa

Degree of Improvement = Pre-treatment Compactness divided by Post-treatment Compactness

#### 4. ENVIRONMENTAL ISSUE

The prime environmental issue of dynamic compaction techniques is its induced vibrations which can cause inconveniences to peoples and, if carelessly conducted, can even cause damages to surrounding structures. Therefore, during dynamic compaction trial test, it is highly suggested to monitor the induced vibration with a modern vibration monitoring instrument which is able to measure the horizontal and vertical vibration acceleration, velocity and displacement / amplitude. The result of the monitoring can then be plotted into vibration hazard criteria presented in Figure 15. With this, measures can be designed to alleviate detrimental effect during the execution of the work.

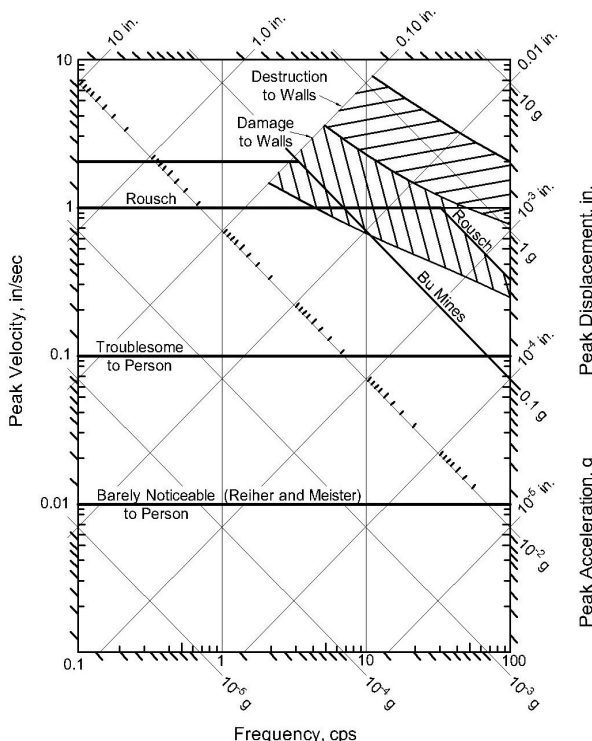


Figure 15 Vibration Hazard Criteria (Richart et al, 1970)

#### 5. CASE HISTORIES

##### 5.1 Dynamic Compaction on Reclaimed Sandy Soils

The project was located in a small town of Lhokseumawe in North Sumatra, Indonesia. The site was originally tidal flatlands adjacent to the beach, with small tidal rivers flowing through the area. During the late 1970s and early 1980s, sandy material dredged from the harbor was pumped to fill the project site. The grade in this area was, thus, raised from near mean sea level to a level approximately 4 m above sea level. A LNG tank of 70 m diameter and 26m high were going to be built side by side. The soil investigation revealed that up to about 30 m depth, the soil was primarily poorly-graded, medium to fine grained, sands in the upper 10 m then grades to only fines with increasing depth. Thin clayey sand layer of about 1 m thick was found at a depth of about 3 to 6 m depth. At this depth the fines (% passing #200 sieve) content was around 30%, whereas at other depths the fine content was generally in the order of 5-15%. Figure 16 shows the soil profile and the SPT blow counts. The site is located at the earthquake prone area, with an anticipated maximum ground surface acceleration of 0.18g. Based on liquefaction potential analysis developed by Seed et al (1982, 1985), the foundation soil was clearly prone to liquefaction. Ishihara (1985) reported that during Niigata Earthquake of 1964, no liquefaction occurred at depth deeper than 15 m. Therefore, it was decided to densify the soil up to 16 m depth by dynamic compaction techniques.

The dynamic compaction was carried out by dropping a 16 ton pounder with contact area of 2 m x 2 m, from 25 m height. The poundings were carried out in two phases. Phase 1 with a grid pattern of 8 m x 8 m. Phase 2, also with a grid pattern of 8 m x 8 m, was carried out at the centre points of the first phase grids. The radius of the improvement, Ri, was taken as radius of the tank, Ro, plus two third of the target improvement depth, D.

$$R_i = R_o + 0.66 D \quad (6)$$

$$= 35 + 0.66 \times 16 = 45.6 \text{ m}$$

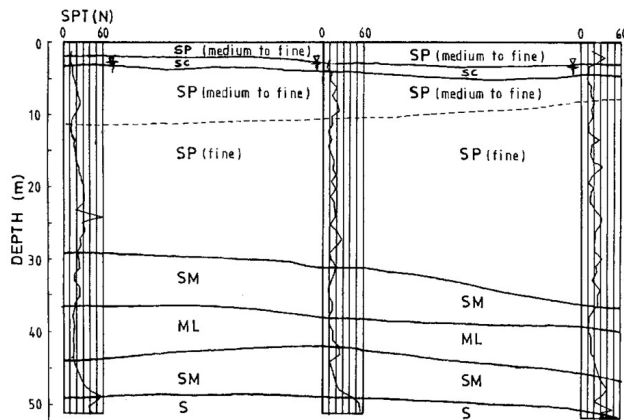


Figure 16 Soil Profiles and SPT Blow Counts at LNG Tank Site

Figure 17 shows the executed tamping pattern. Upon completion of phase 2, the ground surface was further compacted by ironing tamping using the same pounder but with a drop height of only 5m. Cumulative compaction energy applied at the side was 200 t.m/m<sup>2</sup> or 12.5 t.m/m<sup>3</sup> (200 t.m/m<sup>2</sup> divided by improved depth of 16 m). The enforced settlement recorded was within 22 to 28 cm.

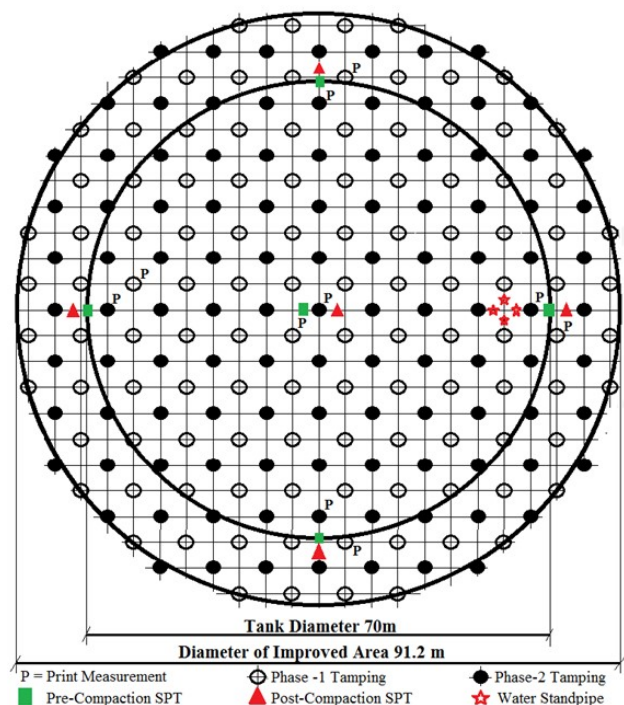


Figure 17 Dynamic Compaction Pattern at LNG Tank Site

Figure 18 shows the pre-compaction vs post-compaction SPT blow counts. It can be seen that only 5 post-compaction SPT data points still falls below the liquefaction boundary line, and majority falls above the boundary line. Those few SPT blow counts that still fall below the liquefaction boundary was judged to be non-significant. The distribution of the SPT N values shows that the impact of dynamic compaction is diminishing with depth. Figure 19 shows the degree of improvement achieved. It can be seen that no improvement was achieved when the pre-compaction normalized SPT N value, ( $N1_{60}$ ), is larger than 30.

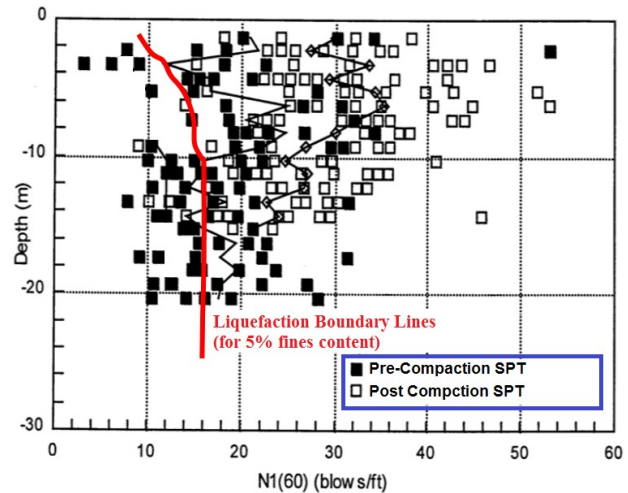


Figure 18 Pre and Post Dynamic Compaction SPT at LNG Tank Site

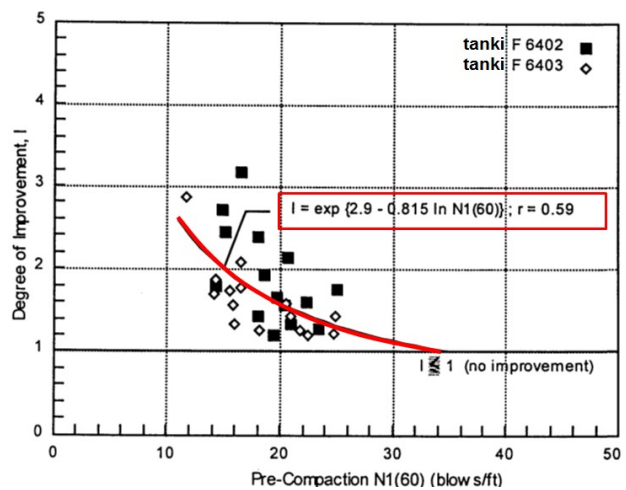


Figure 19 Degree of Improvement Achieved at LNG Tank Site

## 5.2 Dynamic Compaction on Coralline Soils

At Tarahan, South Sumatra, Indonesia, a coal terminal was going to be built. Soil investigation results revealed that the underlying soils consisted of 0.5-4.0 m thick fill material, composed of a mixture of cobble, gravel, sand and silt, overlying 12-16 m thick coralline soil (Figure 20). The coralline soil composed of loose silty sand with substantial amount of coral fragments throughout the depth. The upper 5 m, on average, contained about 30% coarse coral fingers (percent retained in sieve no. 4) while the lower part had about 20%. This coralline soil was underlain by stiffer strata of clayey soil followed by conglomerate in the northern area and stiff to hard clay in the southern area. The water table varied from 1.5 m to 2.5 m depth from the northern to the southern part. The site is located in earthquake prone area. Liquefaction analysis with maximum horizontal ground acceleration of 0.25g and earthquake magnitude of 7.5 showed that the site was prone to liquefaction (Figure 21).

Dynamic compaction was chosen to compact the subsoil up to 10 m depth. A 15 ton pounder with a contact area of 4.3 m<sup>2</sup> and a 20 m drop height was selected. A number of trial compactions were carried out. It was later found that four phases of compaction were needed. Figure 22 shows the compaction pattern. The ironing tamping was conducted with a drop height of 12.5 m. The cumulative energy applied was 295 t.m/m<sup>2</sup>.

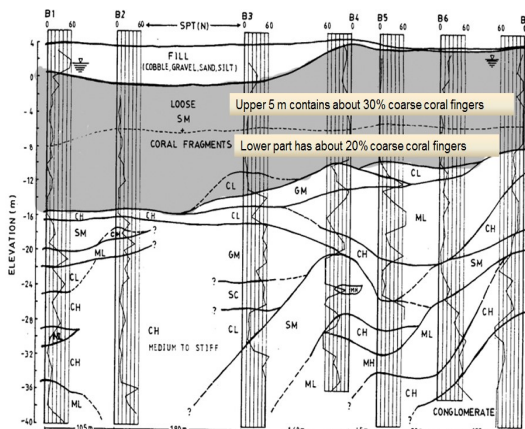


Figure 20 Soil Profile at Coal Terminal Site

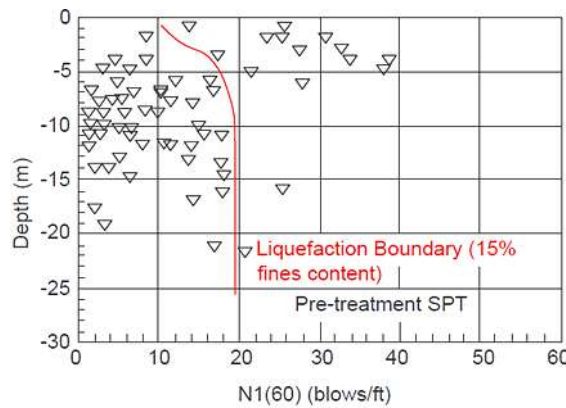


Figure 21 Liquefaction Potential at Coal Terminal Site

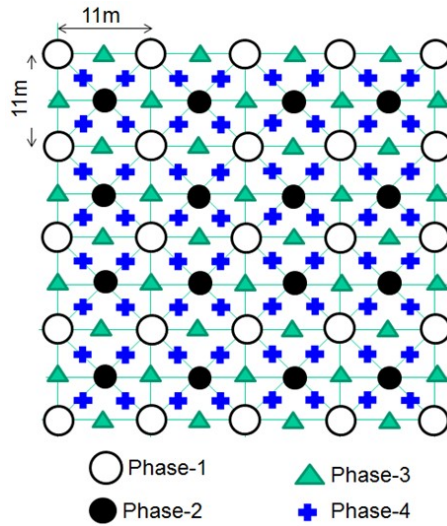


Figure 22 Dynamic Compaction Pattern at Coal Terminal Site

The compaction energy was able to induce enforced settlement of around 70 to 90 cm. However, comparison of pre and post compaction SPT (Figure 23) clearly showed the improvement depth achieved was less than 5 m, which was way off target of 10 m depth. Analysis showed that the compaction could not improve the soil with pre-compaction SPT higher than 20 blows/ft (Figure 24). The applied cumulative compaction energy per unit volume of soil improved was 59 t.m/m<sup>3</sup> (total energy applied at the surface of 295

t.m/m<sup>3</sup> divided by the 5m depth improved). This value was certainly out of the usual range of 20 to 30 t.m/m<sup>3</sup> to compact granular soils.

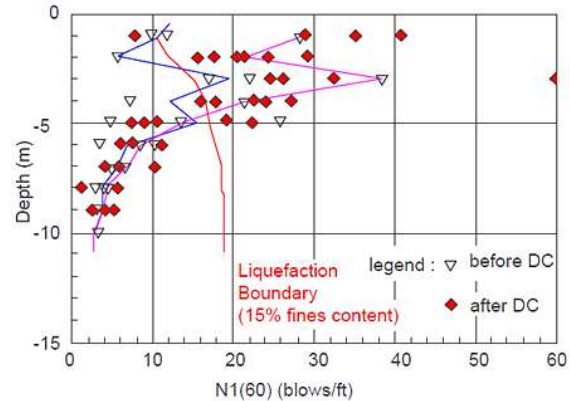


Figure 23 Pre and Post Compaction SPT at Coal Terminal Site

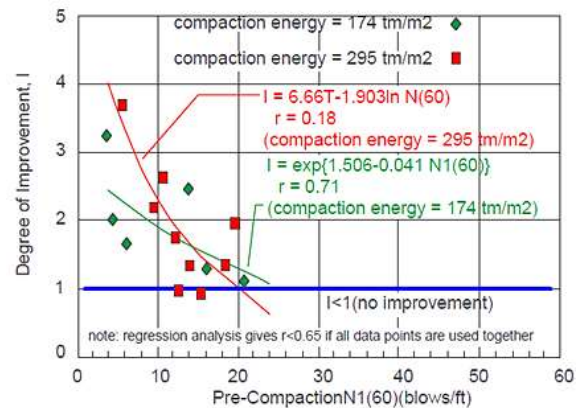


Figure 24 Degree of Improvement Achieved at Coal Terminal Site

Therefore, investigation was carried out. Pre and post compaction grain size distribution of the subsoils revealed that the percentage of fine content increases (Figure 25). Careful visual examination on pre and post treatment soil samples used for grain size analysis showed that the post compaction coral fingers reduce significantly. It was concluded that significant part of compaction energy was absorbed to crush the coral fingers. It was later decided to compact deeper layer by vibro-compaction with added backfill, i.e. to form sand compaction piles.

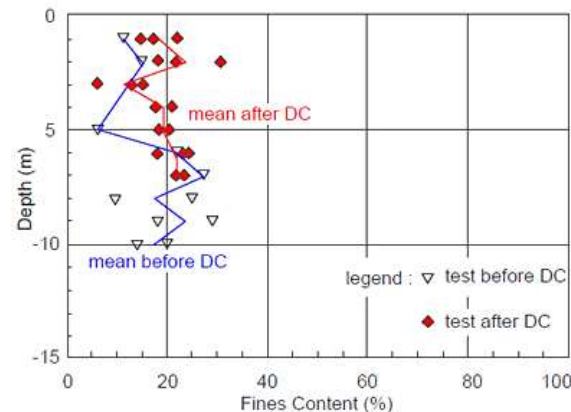


Figure 25 Pre and Post Treatment Fine Content at Coal Terminal Site

### 5.3 Conclusions on the Case Histories

Both case histories show that the degree of improvement achieved by dynamic compaction diminishes with depth. This phenomenon is not exceptional because the fact is the compaction energy transferred to the soil is also diminishes with depth.

Coralline silty sand deposits, i.e. sandy soil with existence of coral fingers, need much higher cumulative compaction energy to compact compared to sandy soil with no coral fingers ( $59 \text{ t.m/m}^3$  vs  $12.5 \text{ t.m/m}^3$ ). About half of the dynamic compaction energy was absorbed to crush the coral fingers. Back calculation of dynamic compaction empirical coefficient  $n$  as in equation (3) showed a low value of only  $0.3$  [ $n = 5 / \sqrt{(15 \times 20)}$ ] to improve the coralline soils compared to a high value of  $0.8$  [ $n = 16 / \sqrt{(16 \times 25)}$ ] to improve the reclaimed sandy soils with no coral fingers. It can be concluded that dynamic compaction is not very effective to improve coralline soils.

### 6. CLOSURES AND ACKNOWLEDGEMENT

This paper is intended as a guideline for practicing engineers to design, execute, and evaluate dynamic compaction ground improvement scheme. The author realized that the write up may not be complete let alone perfect, therefore, feedback from readers are most welcome. Finally, the author would like to thank Prof. A.S. Balasubaramaniam and the committee of SEAGS 50<sup>th</sup> Anniversary Symposium for inviting the author to present this paper.

### 7. REFERENCES

- Andus, R.D. and Stokoe, K.H. (1999) A Liquefaction Evaluation Procedure Based on Shear Wave Velocity, Proc. Joint Meeting US/Japan Natural Resources Development Program, Tsukuba, Japan.
- Cetin, K.O., Seed, R.B., Der Kiureghian, A., Tokimatsu, K., Harder, L.F., Kayen, R.E., and Moss, R.E.S. (2004) SPT-Based Probabilistic and Deterministic Assessment of Seismic Soil Liquefaction Potential, J. Geotech. and Geoenv. Engrg., ASCE, Vol. 130(12), pp.1314-1340.
- Gambin, M.P. (1979) Menard Dynamic Consolidation, Ground Reinforcement Seminar., Washington.
- Gouw, T.L. (1989) Deep Compaction for Ground Improvement and for Reduction of Liquefaction Potential in Sumatra, Indonesia, M.Eng Thesis, Asian Institute of Technology, Bangkok.
- Gouw, T.L., Irsyam, M., Gunawan, A. (2013) The Application of Ground Improvement Techniques in Indonesia, 18th Southeast Asian Geotechnical & Inaugural AGSSEA Conference, Singapore.
- Idriss, I.M and Boulanger, R.W. (2004) Semi-empirical Procedures for Evaluating Liquefaction Potential During Earthquakes, Proc. of 11th ICSDEE and ICEGE, Berkeley, California, USA., pp. 32-56.
- Ishihara, K. (1985) Stability of Natural Deposits during Earthquake, Proc. 11th ICSMFE, (1), 249-252, Tokyo.
- Irsyam M., (2012) Personal Communication.
- Lukas, R.G. (1995) Geotechnical Engineering Circular No. 1 – Dynamic Compaction, FHWA-SA-95-037, Federal Highway Administration, Washington.
- Menard, L. and Broise, Y. (1975) Theoretical and Practical Aspects of Dynamic Consolidation, Geotechnique (25), 3-18.
- Richart, R.E., Hall, J.R., Woods, R.D., (1970) Vibrations of Soils and Foundations, Prentice Hall Inc., New Jersey
- Seed, H.B and Idriss, I.M. (1971) Simplified Procedure for Evaluating Soil Liquefaction Potential, J. Geotech. Engrg., ASCE, Vol. 97 (9), pp.1249-1273.
- Seed, H. B., and Idriss, I. M. (1982) Ground Motions and Soil Liquefaction during Earthquakes, Monograph No. 5, Earthquake Engineering Research Institute, Berkeley, California, pp. 134.
- Seed H.B., K. Tokimatsu, L.F. Harder, and Riley M. Chung (1985) Influence of SPT Procedures in Soil Liquefaction Resistance Evaluations, J. Geotech. Engrg., ASCE, Vol. 111(12), pp.1425-1445.
- Smolcicky, U (1983) Deep Compaction, Proc. 8th European Conference on Soil Mechanics and Foundation Engineering, Helsinki, Vol 3, 1105-1114.
- Soletanche Bachy (2011), Technical Guide, Rueil-Malmaison, France, pp. 103.
- Stark, T. D., and Olson, S. M. (1995) Liquefaction Resistance Using CPT and Field Case Histories, Journal of Geotechnical Engineering, ASCE, vol. 121, no. 12, pp. 856-869
- Qian, J.H. and Qian, Z. (1986) Application of Several Soil Improvement Methods in China, Proc. Int. Conf. Deep Found., Beijing, (2), 1.27-1.34.
- Van Impe, W.F. (1989) Soil Improvement Techniques and their Evolution, Balkema, Rotterdam.